Biomaterials Science

ROYAL SOCIETY OF CHEMISTRY

PAPER

View Article Online
View Journal | View Issue



Cite this: *Biomater. Sci.*, 2023, **11**, 4226

# A chitosan-based self-healing hydrogel for accelerating infected wound healing†

Haohao Cui,[a,b] Bingbing Cui,[a,b] Huiying Chen,[a,b] Xiwen Geng,[a] Xingchen Geng,[a] Zhanrong Li,[a] Shaokui Cao,[b] Jianliang Shen *[c,d] and Jingguo Li *[a,b]

Received 13th January 2023,
Accepted 23rd February 2023

DOI: 10.1039/d3bm00061c

rsc.li/biomaterials-science

Wound infection causes irregular tissue closure, often with prolonged healing. Traditional therapies based on antibiotic delivery have resulted in reduced therapeutic efficiency and drug resistance. Such features make it highly desirable to develop an antibiotic-free material for wound infection in clinical applications. Herein, a self-healing antibacterial hydrogel was designed to realize the treatment of *S. aureus*-infected wounds. The design of the dynamic imine bond endows hydrogels with self-healing and adaptive properties, which could cover the irregular wound and improve the safety of administration. In addition, benefiting from quaternized chitosan, the designed hydrogels also present fascinating antimicrobial properties and favorable biocompatibility. The evaluation in a rat skin wound infection model indicates that the fascinating antimicrobial effect accelerates wound healing by the designed hydrogels. This facile design of an antibiotic-free material allows effective wound infection management, which may be promising in coping with other complex wound healings.



## Introduction

The skin constitutes an important organ that covers the surface of the human body and combines extreme mechanical features with sensing abilities, which play diverse roles such as regulating body temperature and preventing humans from the invasion of harmful substances.[1–3] However, the skin will lose the most protective effect because of the existence of wounds in direct contact with the external environment. Despite the fact that most common injuries can be restored to their original appearance *via* a wide range of biological events including homeostasis, inflammation, proliferation and remodeling, an infection caused by microbial invasion is hardly controllable without effective intervention.[4–7] Excessive inflammation and tardy cell proliferation processes accompanying an abnormal wound recovery such as prolonged healing, the growth of wound size and tissue decay.[8–10] The past few decades have witnessed the effects of antibiotics and a great deal of efforts such as antibiotic-encapsulated delivery have also been widely explored, but inevitably drug resistance occurs.[11–14] The reduced therapeutic efficiency cannot efficiently cope with microbial invasion in the processing of wound closure.[13] Therefore, it is desirable to tailor a novel facile and competitive antibiotic-free system that facilitates wound repair.[15]

Hydrogels, based on natural polymers, have emerged as promising candidates due to their excellent wound exude absorbance capacity, shape adaptability, moisture-retaining nature and biocompatibility.[16–22] In particular, hydrogels can cover the wound and provide a platform for the recruitment of epithelial cells and deposition of collagen and then promote tissue regeneration.[3,23–27] However, endowing hydrogels with antimicrobial activity, inorganic metal ions,[28–33] antimicrobial peptides,[34] and polyphenols[6,35] are often involved. These designs exhibit fascinating antibacterial capacity with or without external factors such as light, $O_2$, and so on.[36,37] Unfortunately, considering potential factors, tissue lesions because of the aggregation of metal ions, external stimuli and irreversible oxidation of phenols, such materials result in unsatisfactory antibacterial activity. Various photothermal agents have also been incorporated into polymer networks,[38–41] however, photothermal sterilization may arise toxin accumulation and excessive inflammation in tissues,

[a]*Henan Provincial People's Hospital, People's Hospital of Zhengzhou University, Zhengzhou 450003, China. E-mail: lijingguo@zzu.edu.cn*
[b]*School of Materials Science and Engineering, Zhengzhou University, Zhengzhou 450001, China*
[c]*School of Ophthalmology and Optometry, School of Biomedical Engineering, Wenzhou Medical University, Wenzhou 325027, China. E-mail: shenjl@wibe.ac.cn*
[d]*Wenzhou Institute, University of Chinese Academy of Sciences, Wenzhou 325001, China*

†Electronic supplementary information (ESI) available: Characterization, scanning electron microscopy (SEM) analysis, rheological studies, swelling behavior, antimicrobial capacity evaluation, biosafety assays and an *in vivo* infected full-thickness skin defect model, schematic diagram of the synthesis of QCS and PEGDA, illustration of the nature of self-healing hydrogels, Fourier transform infrared (FTIR) spectra of QCS, PEGDA and QP hydrogels, $G'$ and $G''$ values of the hydrogels on frequency sweeps, cytotoxicity of L929 cells incubated with $QCS_{0.25}$ and $QCS_{0.5}$, and the cytotoxicity of L929 cells incubated with the hydrogels. See DOI: https://doi.org/10.1039/d3bm00061c

thus causing delayed wound closure.[42,43] Besides, traditional hydrogel dressings have increasingly shown their limitations, with no healing, poor shape matching, and weak wound retention capacity. Therefore, the development of a biocompatible, adaptive, self-healing, antibacterial and moderate adhesive hydrogel system is promising in infected wound healing.

Chitosan, a natural cationic polymer, shows powerful performances of biocompatibility, biodegradability, antibacterial capability, and hemostasis, which can promote the whole process of wound healing.[44–46] However, the limited water solubility hinders its further application in the research and development of antibacterial hydrogel dressing. Chitosan modified with quaternary ammonium polymers demonstrated good biocompatibility, better water solubility and enhanced antimicrobial activity.[47,48] These desired traits indicate that quaternized chitosan (QCS) has promising application prospects as an antibacterial agent. Besides, polyethylene glycol (PEG), a synthetic polymer, has also been widely used for its biosafety and hydrophilic properties and previous studies often focus on the preparation and bioactivities of water-soluble functions of PEG derivatives.[49,50]

In addition, hydrogels with self-healing capacity could emulate the dynamic structural features of extracellular matrices, which could provide support and prevent the adverse consequences caused by gel rupture.[51,52] A hydrogel design based on dynamic chemical bonds, *e.g.*, disulfide bonds, phenylboronic ether, imines and so on, allows the reversible regulation of hydrogel structures and perform on-demand actuation, which is conducive to clinical applications.[53–55] However, the reported antibacterial activity of hydrogels was limited to the surface area, and antibacterial agent solutions are not long-acting and need multiple dosing. Given these traits, a dynamic hydrogel system consisting of biocompatible polymers entirely was designed and developed. QCS was selected to react with the PEG derivative (dialdehyde terminated PEG), named PEGDA, to form a three-dimensional hydrogel network. The proportion of crosslinking agents was reduced to form a system susceptible to acid hydrolysis and combine the merits of hydrogels and solutions. Smart hydrogels, based on natural polymers, combine the advantages of self-healing, antibacterial and antibiotic-free properties, showing favorable properties different from other studies which focus on one or several of these properties. The biocompatible, adaptive, self-healing, antibacterial, and moderate adhesive properties, and physicochemical features of the designed hydrogels were evaluated *in vitro*. Additionally, a rat skin wound model was also used to analyze the antimicrobial capacity and the ability to accelerate wound recovery.

# Results and discussion

### Preparation and characterization of dynamic hydrogels

A schematic representation of antibacterial hydrogels is shown in Scheme 1. First, QCS was synthesized by grafting glycidyl trimethylammonium chloride (GTMAC) on the backbone of hydrophilic chitosan (Scheme S1A, ESI†) and confirmed by $^1H$ NMR and FTIR spectroscopy (Fig. 1A and C). The peaks at 3.1 and 3.3 ppm were assigned to the trimethylammonium groups and –NH–$CH_2$– groups. In the FTIR spectra, the peak at 1475 $cm^{-1}$ was assigned trimethylammonium, suggesting the successful preparation of QCS. Similarly, PEGDA was synthesized by an esterification reaction of PEG with 4-carboxybenzaldehyde (Scheme S1B, ESI†). The peaks of ester methylene, the benzene ring, and the aldehyde group were detected in the $^1H$ NMR and FTIR spectra (Fig. 1B and D), indicating that the aldehyde group was modified to the PEG terminus. These results demonstrate that the designed precursor polymers were obtained.

Dynamic hydrogels were developed by the combination of two different precursor solutions. QCS was dissolved in phosphate buffered saline (PBS) buffer at a concentration of 3.3, 4.4 and 5.5% w/v, respectively. When mixing the QCS solution with the PEGDA solution, the mixture underwent a sol-to-gel transition in a short period to form a dynamic hydrogel with PEGDA as a cross-linker (Schemes S1 and S2†). The final concentrations of QCS are 3, 4, and 5% w/v, and that of PEGDA is 1% w/v. The hydrogels obtained were denoted as QP-1, QP-2, and QP-3. The FTIR result showed the occurrence of imine bonds, suggesting the successful formation of dynamic hydrogels (Fig. S1, ESI†).

### Physicochemical properties of the hydrogels

Moderate mechanical strength is essential for fabricating wound dressings to maintain their structure and cover wound surfaces.[45] So, rheological experiments were conducted to study the mechanical behavior of all hydrogels, and the storage modulus ($G'$) and loss modulus ($G''$) were detected on a rheometer to evaluate the viscoelasticity of the samples. It was found that the $G'$ values increase from 15.8 Pa to 120 Pa with an increased concentration of QCS, indicating enhanced mechanical strength with more QCS (Fig. 2A).

Besides, it was accepted that as a wound dressing, hydrogels could absorb wound exudates and provide a moist environment. Thus, the equilibrium swelling rate (ESR) of all hydrogels was investigated in PBS at room temperature. In Fig. 2B, the ESR of dry hydrogels decreased dramatically as the concentration of QCS increased and QP-3, containing the highest concentration of QCS, showed the lowest ESR compared to other groups. This was determined by its tighter crosslinking network and closer crosslinking density.

Each hydrogel sample was also lyophilized to investigate the morphology through SEM. The results indicated that the prepared hydrogels have porous structures and a relatively homogeneous distribution (Fig. 2C). The variation in pore size can be attributed to increased crossing density, suggesting their uniform chemical interactions, which is consistent with the storage modulus and ESR results.

### Self-healing, adaptive and adhesive properties of the hydrogels

External mechanical forces and traction generated by body movement may damage the integrity of the hydrogels to a

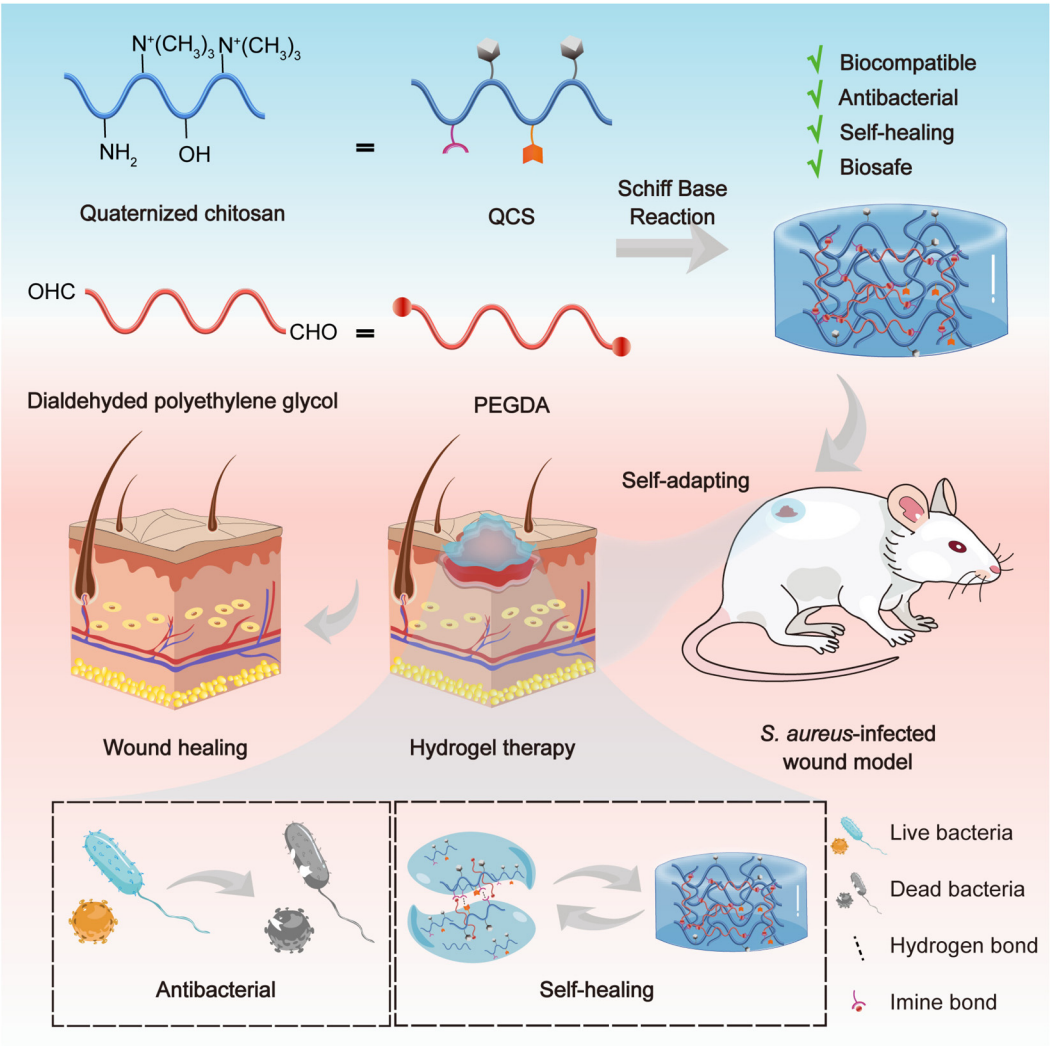


**Scheme 1** Schematic illustration of the preparation and application of a dynamic antibacterial hydrogel.

certain extent and then affect the function and service safety.[26,29] Therefore, hydrogels with favorable self-healing ability and shape adaptive behavior are essential in wound closure due to the dynamic nature of cross-linking. The design strategy was based on an imine bond, which could readily form under physiological conditions and respond to environmental pH changes. To estimate the self-healing behavior of the hydrogels, QP-1 was chosen to model the sample to conduct subsequent tests. A frequency sweep test was first conducted at a frequency of 1 rad per s with an applied strain above 158%; the $G''$ value exceeded the $G'$ value, revealing the breakdown of the hydrogel structure (Fig. 2D). Therefore, a cyclic strain test was conducted with the oscillatory strains alternatively switched from 10% to 250% (Fig. 2E). When a high dynamic strain (250%) was applied, the value of $G'$ was lower than that of $G''$, suggesting the breakdown of the hydrogel structure. When a lower strain (10%) was applied, the value of $G'$ was restored to its original value after four alternative cycles, which indicates the self-healing ability of the hydrogels.

Next, a macroscopic healing test was performed to assess the self-healing capacity. For a clearer observation, the hydrogels were dyed blue and red, and placed together at ambient temperature to enable the recovery of the hydrogels without any external intervention (Fig. 2F). It was found that the healed hydrogels hold together evenly with no cracks. In addition, the hydrogels can slowly fill irregular areas and join together as a whole, which is determined by the fluid nature and dynamic bond of the hydrogels with weak shear frequencies (Fig. 2G and Fig. S2†). All these traits indicated that the designed hydrogels possess favorable self-healing ability, which could be attributed to the imine bond and hydrogen bond in the QCS network.[56]

Similarly, a hydrogel with moderate adhesive capacity could adhere to skin wounds without any intervention, which provides a good healing environment. The adhesive properties of the designed hydrogel were investigated by adhering to different surfaces such as metals, paper, wood, plastic, glass, and skin (Fig. 2H). The underlying mechanism can be attribu-

 

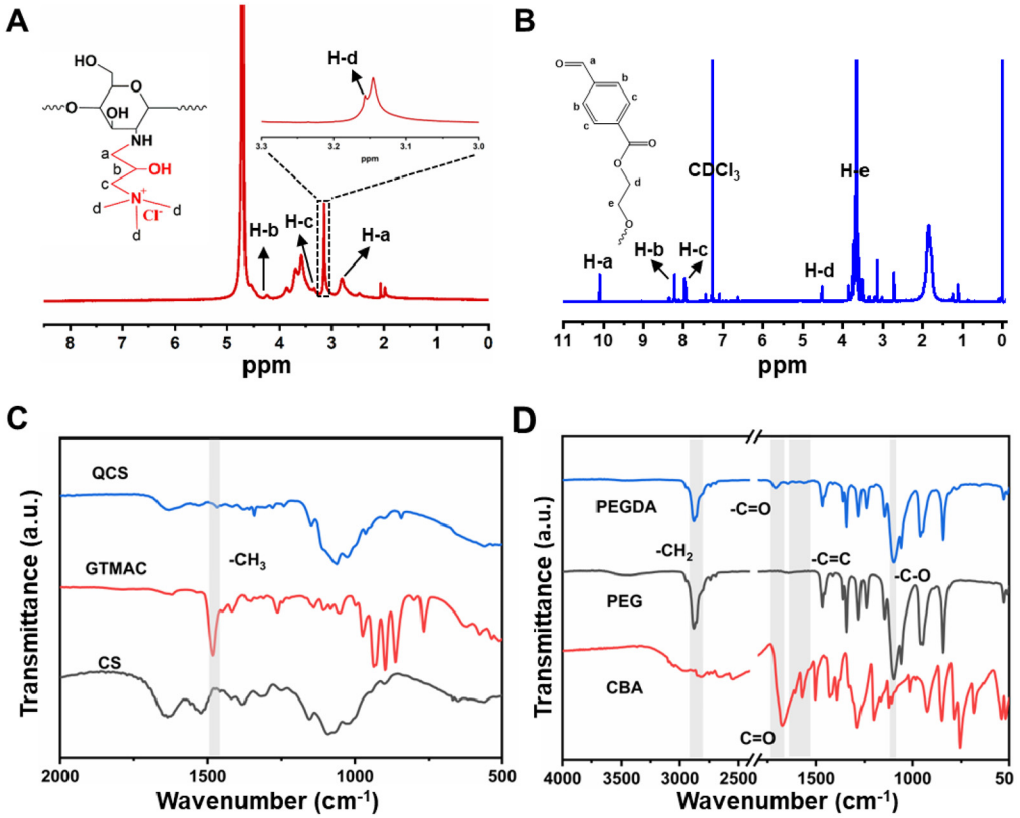


**Fig. 1** Characterization of QCS and PEGDA. $^1H$ NMR spectra of QCS (A) and PEGDA (B). Fourier transform infrared (FTIR) spectra of QCS (C) and PEGDA (D).

ted to the charge interaction of QCS with various negatively charged surfaces. This means that the designed hydrogels can remain at the lesion site for a longer time, which is conducive to wound healing.

### Antibacterial activity *in vitro*

Gram-positive (*S. aureus*) and Gram-negative (*E. coli*) bacteria were chosen to investigate the antibacterial activity of the designed materials. First, the antimicrobial ability of three QCS samples with different degrees of substitution, named $QCS_{0.1}$, $QCS_{0.25}$, and $QCS_{0.5}$, respectively, was evaluated using 3-(4,5-dimethylthiazol-2-yl)-2,5-diphenyl tetrazolium bromide (MTT). The more the bacteria, the stronger the chromogenic reaction. The susceptibility of three samples to two bacteria, *S. aureus* and *E. coli*, was tested using chitosan as a positive control. The minimum inhibitory concentration (MIC) was defined as the minimum concentration of the drug used for bacterial survival below 10%. The results are shown in Fig. 3A and 4A and the MIC indicated that QCS was more sensitive to *S. aureus* compared with chitosan. The higher the substitution degree, the better the antibacterial capacity. The MIC of $QCS_{0.5}$ for *S. aureus* was less than 4 μg $mL^{-1}$. Although QCS is not as sensitive to *E. coli* as to *S. aureus*, it still has a fascinating bactericidal effect at a concentration of 312 μg $mL^{-1}$. Therefore, $QCS_{0.25}$ and $QCS_{0.5}$ were chosen for subsequent biosafety experiments. Their preliminary cytocompatibility and cell viability were measured to evaluate their biosafety as shown in Fig. S3.† Compared with $QCS_{0.5}$, $QCS_{0.25}$ has a higher cell survival rate at a certain concentration of 4 mg $mL^{-1}$, suggesting excellent biocompatibility. Thus, $QCS_{0.25}$ was chosen as the targeted polymer to fabricate a hydrogel system.

QP hydrogels were brought in contact with bacteria to test their surface antibacterial capacity. After incubation with *S. aureus* at 37 °C for 1 h, there was no bacterial colony of all groups (Fig. 3B). This was because the cationic hydrogels could disintegrate bacterial membranes in terms of cationic interactions, making the bacteria lose their proliferation ability. As for *E. coli*, few colonies appeared (Fig. 4B). It is speculated that Gram-negative bacteria are not susceptible to cationic charge but the hydrophobic effects of QCS and inadequate contact time.[57,58]

SEM was also performed to observe the bacterial morphology. After incubation with the bacteria for 5 h, the *S. aureus* cells showed a damaged, wrinkled, and ruptured membrane structure (Fig. 3C). As for *E. coli*, the permeability of the bacterial cell membrane treated with QP-1 and QP-2 was changed for the sake of the interaction between the cationic gel and the bacteria, but the cell morphology may not change significantly (Fig. 4C). Interestingly, the cell morphology of the QP-3 hydrogel showed collapse of the morphology, which indi-

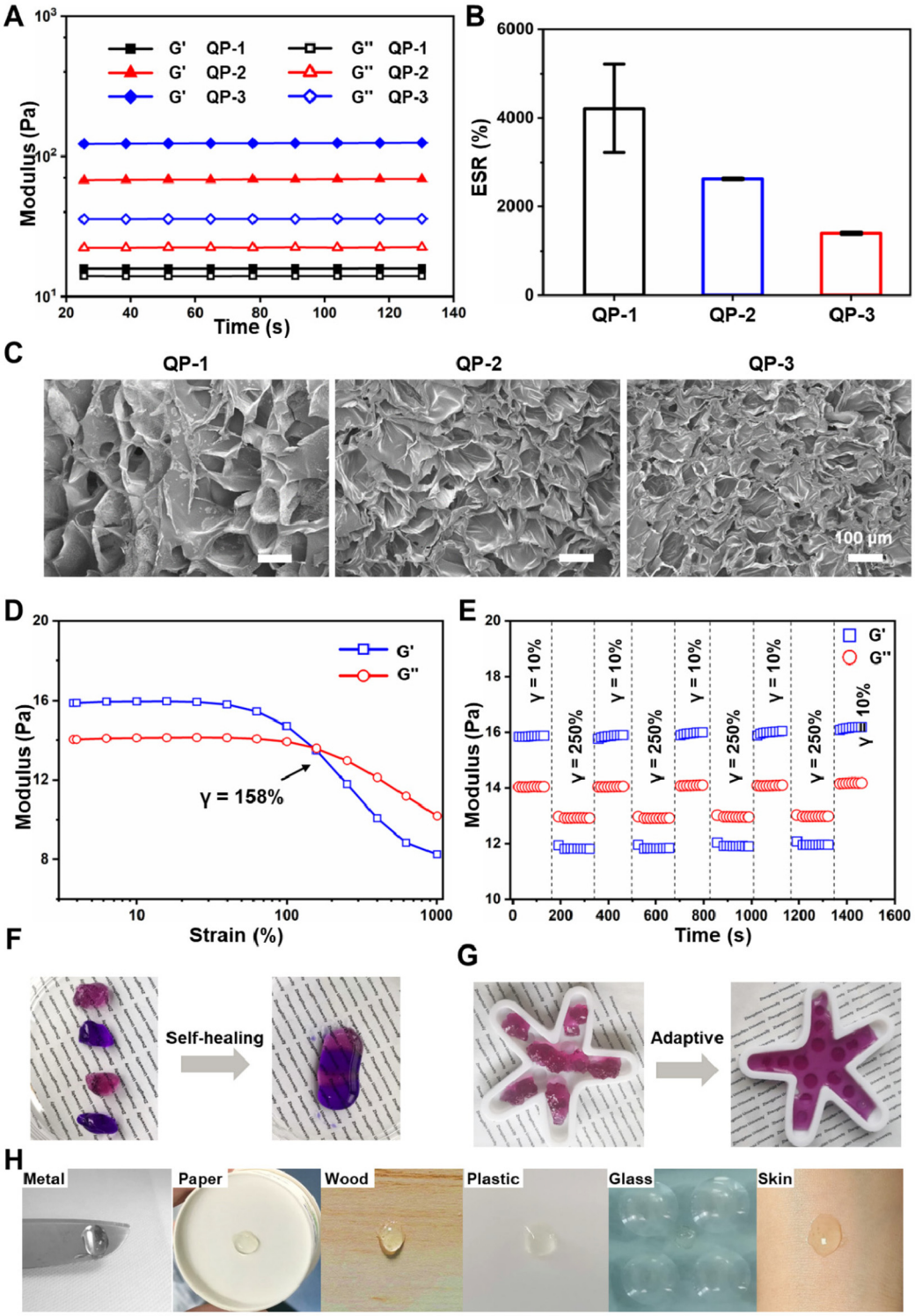


Fig. 2 Characterization of the prepared hydrogels. (A) Rheological behaviors of the gels. (B) Equilibrium swelling rate of the hydrogels. (C) SEM images of the hydrogels. (D) *G′* and *G″* values of QP-1 on an amplitude sweep at 25 °C. (E) Rheological behaviors of the gel with alternative strains switched from 10% to 250% for four cycles. Self-healing (F) and adaptive (G) behavior of the designed hydrogel. (H) Cationic hydrogels adsorbed onto different surfaces.

cated the fascinating antimicrobial capacity of the designed materials. It was speculated that the local acidic environment caused by the bacteria causes the hydrogel breakdown, and the QCS is released. The antibacterial effect depends on the surface of the hydrogel and the free QCS. Since Gram-positive bacteria are more sensitive to the polymer, all groups showed a

 

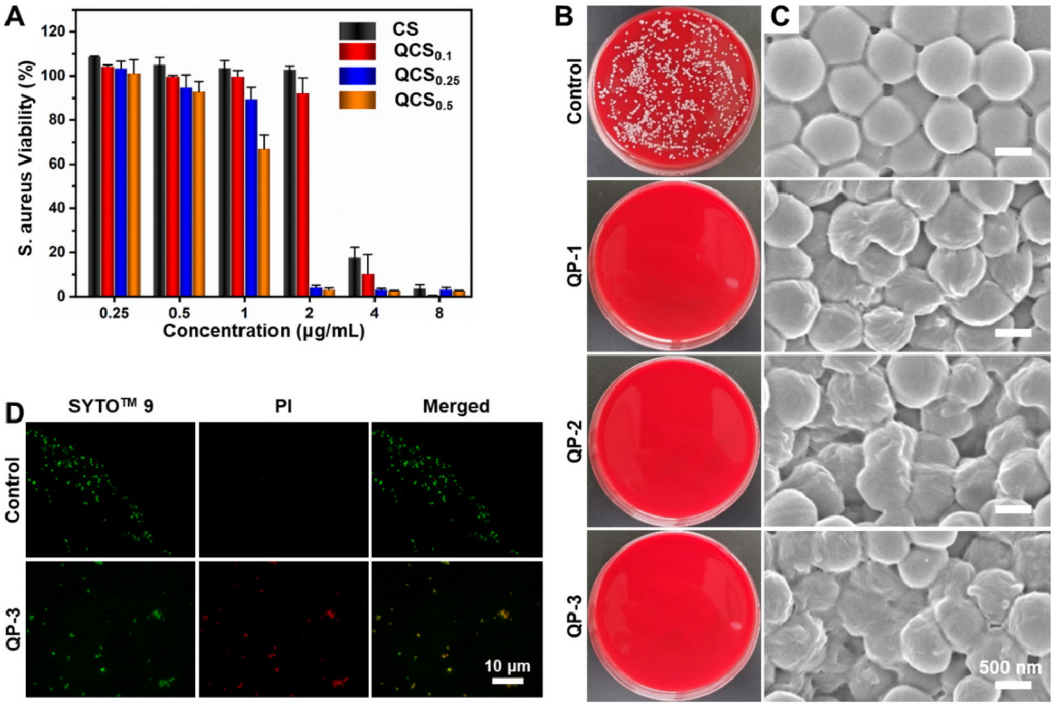


**Fig. 3** Antibacterial activity evaluation of the prepared materials. (A) Bacterial cell viability of *S. aureus* treated with CS and QCS with different grafting rates. (B) Bacterial colonies and (C) SEM images of *S. aureus* with different treatments. (D) Fluorescence images of *S. aureus* after incubation with the QP-3 hydrogel for 2 h.

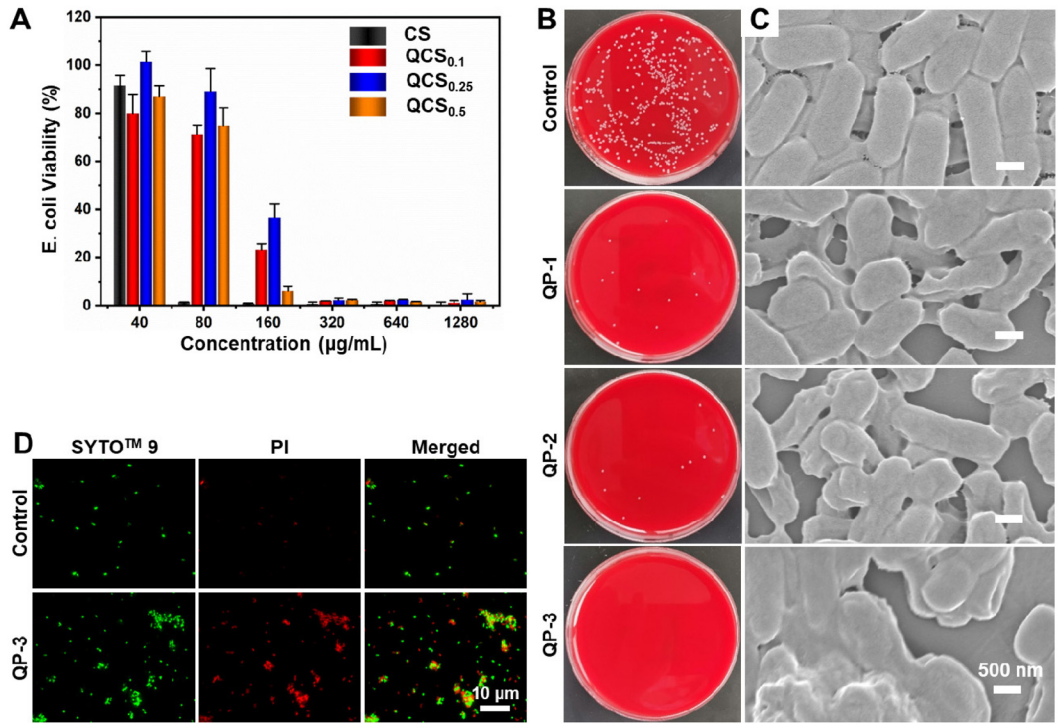


**Fig. 4** Antibacterial activity evaluation of the prepared materials. (A) Bacterial cell viability of *E. coli* treated with CS and QCS with different grafting rates. (B) Bacterial colonies and (C) SEM images of *E. coli* with different treatments. (D) Fluorescence images of *E. coli* after incubation with the QP-3 hydrogel for 2 h.

good effect against *S. aureus*. A fascinating bactericidal effect was also achieved with the increased QCS concentration in terms of *E. coli*. Fluorescence staining tests for live/dead bacterial staining were also conducted. As shown in Fig. 3D and 4D, it was found that most of the cells were green, and only a few dead cells were found in the control group. However, after the hydrogel treatment, the membrane structure of the bacteria was destroyed, and the dead cells occupied the majority. All these results demonstrated that the designed hydrogel exhibited excellent antibacterial activity.

### Biosafety tests of the hydrogels *in vivo*

Biomaterials made from nature or natural derivatives that could resemble living matter are currently promising as they inherit the merits of living matter such as biocompatibility and biodegradability, which differ from those of synthetic polymers.[16,17] Compared to the other research studies (Table S1†), the designed hydrogels combine the advantages of being natural polymer-based, self-healing, antibacterial metal ion-free and antibiotic-free, and serve as long-acting antibacterial and biocompatible wound dressings. However, previous studies focused on one or several of these properties, which are suitable for common wound healing but not for wound infection, for example.[2,5,6,9,27,47,63] In addition, the problem of antibiotic resistance,[11–14] the antimicrobial instability of polyphenols[6,35] and the accumulation of metal ions in wounds[28–30,64] are other factors limiting the further development of most studies. However, herein, chitosan modified with quaternary ammonium salts possesses favorable biocompatibility, improved solubility, and enhanced and long-acting antimicrobial properties.[47,48] The nature of the cationic polymer was the leading factor of membrane breaking sterilization, which did not cause drug resistance and was theoretically biosafe.[57,64,65] Through a facile dynamic strategy of the imine bond, a multifunctional dressing was successfully designed and applied for subsequent experiments.

Biosafety tests were performed by CCK-8 assay in L929 cells. As shown in Fig. S4,† when the hydrogel leaching solution was co-incubated with the cells, the cells in all groups showed a cell survival rate higher than 80%, indicating the favorable biosafety of the designed hydrogels. The QP-3 samples presented the maximum mechanical strength, minimum swelling rate,

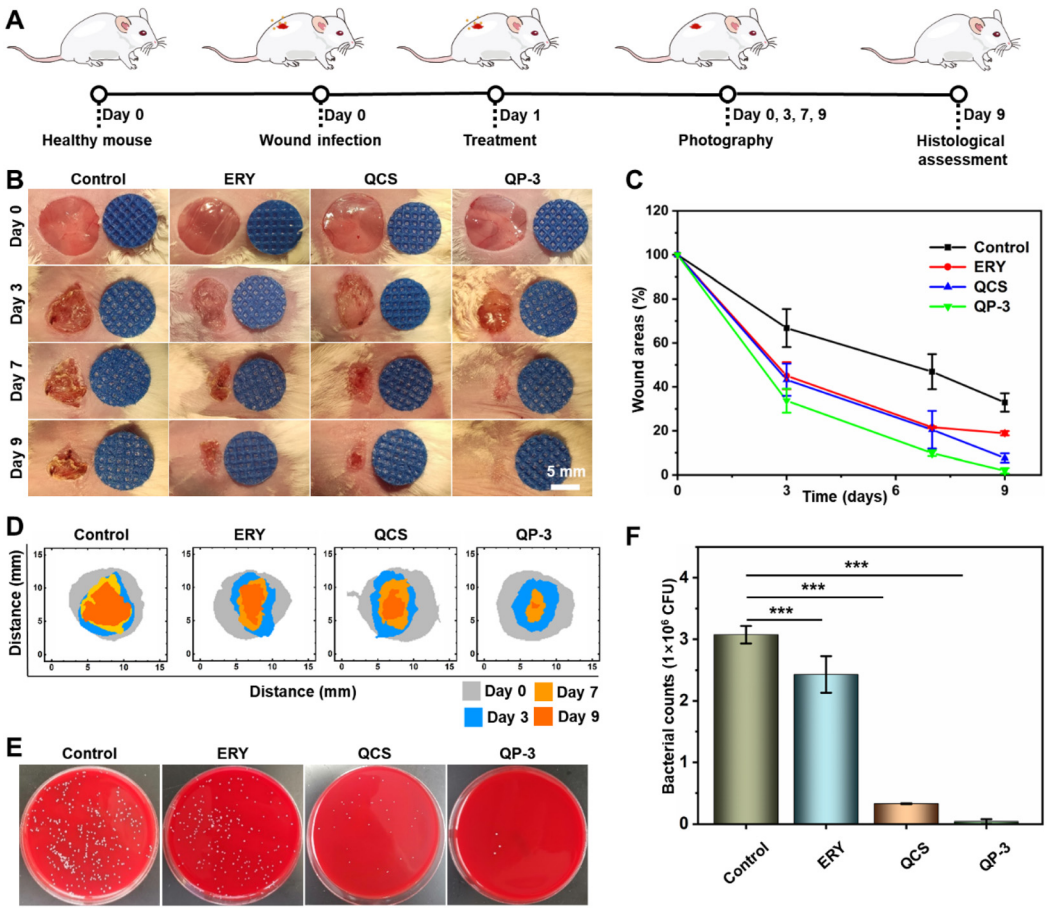


**Fig. 5** *In vivo* treatment of an infected wound model. (A) Illustration of the establishment of an infected wound model and drug administration. (B) Representative photographs of the wounds with different treatments. (C) Images of wounds at different time points and quantitative results. (D) Schematic images of wound contraction over 9 days for ERY, QCS, and QP-3 and wounds with no treatment as a control. (E) Images of survival bacterial clones on day 9 *in vivo*. (F) Bacterial counts in different groups on day 9 *in vivo* (mean ± SD, $n = 3$), ***$P < 0.001$.

 

and favorable biocompatibility, which realized the dynamic balance of materials' properties and they were selected as a candidate material for *in vivo* studies.

### *In vivo* infected wound closure and healing

The antibacterial agent solutions are free to move and can be taken up by cells to exert an antibacterial effect, but they are not long-acting and need multiple dosing. Hydrogel therapy promotes wound healing, but the antibacterial activity is limited to the surface of the material. In this design strategy, the proportion of the crosslinking agents was reduced to form a system susceptible to acid hydrolysis and combine the merits of hydrogels and solutions. The hydrogels exert a surface antimicrobial effect and provide a moist environment for the wound and the free QCS released by the acid hydrolysis played a further bactericidal role. In order to demonstrate our hypothesis, female Balb/c rats were selected to model animals and *in vivo* antibacterial tests were performed. A full-thickness wound infection model, *S. aureus*-induced, was used to estimate the wound closure performance of the QP-3 hydrogel (Fig. 5A). A rough wound (10 mm) was made on the back of the rats. Then a certain amount of bacterial suspension was added to the wound areas to realize infection. After 1 day, incisional wounds were treated with erythromycin ointment (ERY), QCS and QP-3 hydrogel, and the wounds with no treatment were the control (Fig. 5B–D). At the beginning of healing, the wound areas without treatment remain slow in recovery, while wound areas treated with QP-3 become well closed. As for the ERY and QCS groups, wound areas decreased slightly. On day 9, the wound area treated with QP-3 almost disappeared and, in the ERY and QCS groups the wound area became very small and QCS had a better effect compared with the ERY group. But it is noted that the incisions without treatment showed obvious scars after healing.

Besides, plate counting was performed to quantificationally analyze the bacterial levels in the wound sites on day 9 (Fig. 5E and F). The results showed minimal bacterial colonies in the QP-3 group compared to other groups, initially indicating the fascinating antibacterial capacity of the designed hydrogel.

To further evaluate the healing of the wound, histological analysis was conducted on day 9. The aggregation and activation of inflammatory cells and the integrity of tissue morphology are important characteristics of wound healing, which could be observed by hematoxylin and eosin (H&E) staining. As shown in Fig. 6A and Fig. S5,† the skin tissues in the control and ERY groups exhibit a suboptimal tissue repair,

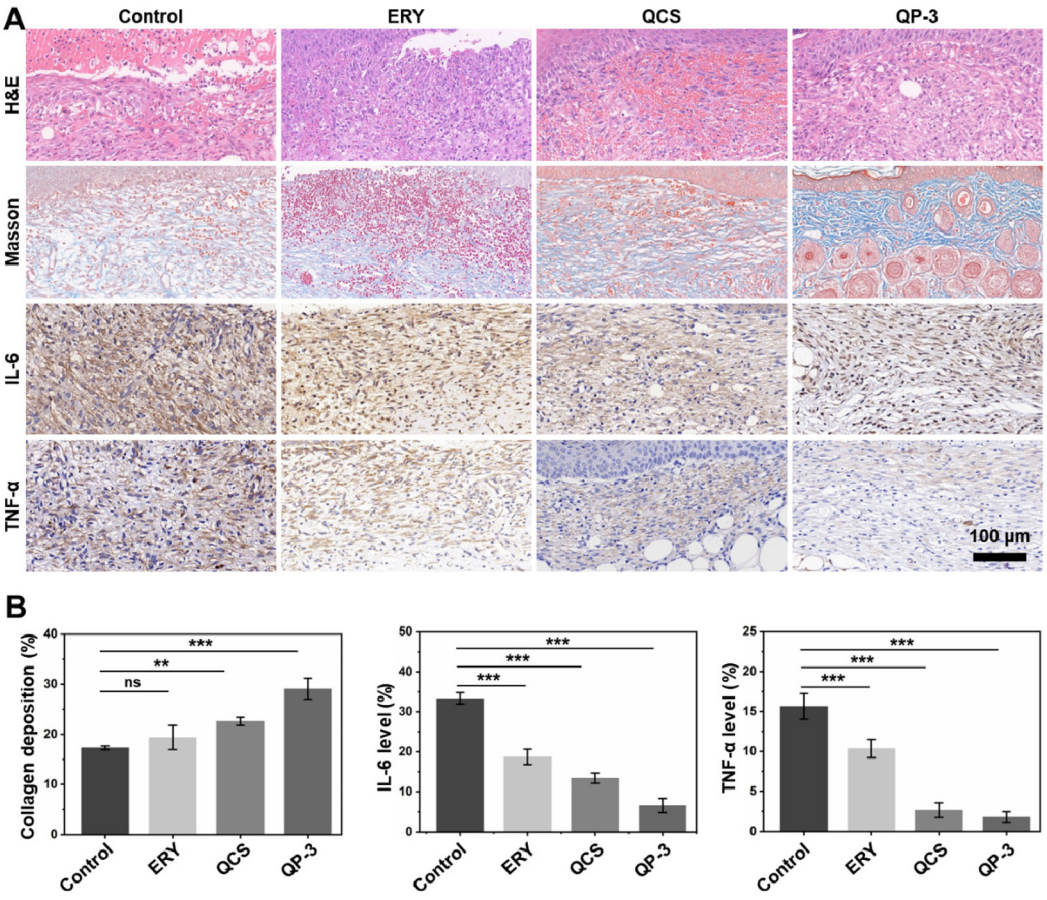


**Fig. 6** (A) H&E staining, Masson trichrome, and immunohistochemical analyses of TNF-α and IL-6 of healed skin tissues on day 9. (B) Quantitative results of collagen deposition, IL-6 and TNF-α (mean ± SD, $n = 3$), $^{**}P < 0.01$, $^{***}P < 0.001$.

while the skin tissue treated with QCS and QP-3 shows an intact tissue structure. Collagen deposition was also evaluated through Masson trichrome staining. The collagen was marked in blue, and the keratin or muscle fibers were marked in red. The results indicated that all groups showed obvious collagen deposition and the QP-3 group showed the best and thickest collagen deposition (Fig. 6A and Fig. S5†). In addition, the protein levels of TNF-α and IL-6 were examined by immunohistochemistry (Fig. 6B). Among all groups, the expression of TNF-α and IL-6 of QP-3 was the most downregulated. This indicated that on day 9, QP-3 expressed the least inflammatory factors, which was attributed to the regulatory effect of QCS. As for the effect of the QP-3 group over the QCS group, it was speculated that the hydrogel could cover the wound better and stay for a longer time, which is conducive to wound closure. This also demonstrated our hypothesis that the design of a low concentration crosslinking agent combines the merits of solutions and hydrogels and thus exerts a fascinating effect. Additionally, the hydrogels with fascinating antibacterial, favorable self-healing and moderate adhesive properties indicate that: (1) the system can remain in the lesion for a longer time; (2) it is in full contact with the wound to provide protection and exert surface antibacterial capacity; and (3) it maintains the integrity of the materials and adaptively cover the whole wound to accelerate wound healing.

## Conclusions

In summary, a smart hydrogel with biocompatible, adaptive, self-healing, antibacterial, and moderate adhesive properties was designed and facilely fabricated through an imine bond. The whole system, consisting of biocompatible materials entirely and without the addition of antibiotics and inorganic metal ions, provides tremendous advantages for infected wound treatment. The results demonstrate that the design of a dynamic network endows the hydrogels with self-healing and adaptive properties, which could cover an irregular wound and improve service safety. The innate antimicrobial capacity of biomaterials makes it promising against bacterial infection without any external intervention, avoiding the occurrence of drug resistance and accumulation of toxic substances. With all these favorable traits, the developed hydrogels are effective in closing wounds and fighting microbial infection, showing promise as a wound dressing.

## Materials

Chitosan with a deacetylation of 85% was purchased from Haidebei Marine Bioengineering Co., Ltd (Jinan, China) and used without further purification. Glycidyl trimethylammonium chloride (GTMAC), 4-carboxybenzaldehyde (CBA), 1-ethyl-3-(3-dimethylaminopropyl) carbodiimide (EDC) and 4-dimethylaminopyridine (DMAP) were purchased from J&K Scientific Ltd (Beijing, China). 3-(4,5-Dimethylthiazol-2-yl)-2,5-diphenyl tetrazolium bromide (MTT) was purchased from Sigma Biochemical Technology Co. Ltd (Shanghai, China). Erythromycin ointment (ERY) was purchased from Xinxiang Huaqing Pharmaceutical Co., Ltd. A LIVE/DEAD™ Baclight™ Bacterial Viability Kit (L7012) was purchased from Invitrogen (China). Cell counting kit-8 (CCK-8) was purchased from Beyotime (China). Dialysis bags (MWCO: 3.5 kDa) were purchased from Shanghai Green Bird Technology Development Co., Ltd. All reagents were of analytical grade and used as received. *S. aureus* (ATCC 29213), *E. coli* (ATCC 25913) and fibroblast L929 cells (ATCC, #CRL-2148) were provided by the microbiology lab of Henan Eye Institute.

### Synthesis of QCS

QCS was prepared according to the literature with a little modification.[45,59,60] Briefly, chitosan (4 g) was dissolved in distilled water (200 mL) with hydrochloric acid at 55 °C to form an aqueous solution. Then 3.08 g of glycidyl trimethylammonium chloride was added dropwise under continuous stirring, which allowed grafting on the chitosan backbone. The molar ratios of GTMAC and amino groups were set as 1 : 10, 1 : 4 and 1 : 2. After stirring for 24 h, the reaction mixtures were filtered to remove the undissolved polymer, and then the solution was transferred into a dialysis bag (MWCO 3500) against deionized water for purification for 3 days and then lyophilized.

### Synthesis of PEGDA

Dialdehyde group-functionalized PEG was synthesized according to the literature.[61,62] Briefly, PEG (4 g, 3350), CBA (0.717 g), EDC (1.1 g), and DMAP (0.06 g) were dissolved in dry dichloromethane in a round-bottomed flask, and then stirred for 24 h. Afterward, the reaction was stopped and the mixtures were concentrated using a rotary evaporator. The resulting products were redissolved and the visible precipitate was removed by centrifugation. Subsequently, the crude products were further purified by dialysis with ultrapure water. After lyophilization, the final product PEGDA was obtained and preserved for further use.

### Hydrogel preparation

In the process of preparing the QP hydrogel, the QCS solution was dissolved in PBS at a concentration of 3.3%, 4.4%, and 5.5% (w/v), respectively, and the corresponding PEGDA solution with a concentration of 11% in PBS was prepared. Then predetermined volumes of QCS and PEGDA solutions were mixed under vigorous stirring. The final hydrogel samples containing 1% (w/v) PEGDA and 3%, 4%, and 5% (w/v) QCS, respectively, were obtained. All hydrogel samples were lyophilized to obtain dehydrated scaffolds for further studies.

## Statistical analysis

Data are shown as the mean ± standard deviation (SD). The statistical trends from different groups were evaluated using

 

one-way analysis ANOVA with LSD's *post hoc* test. Data were expressed as the statistically significant difference when $^{**}P < 0.01$ and $^{***}P < 0.001$.

## Ethical statement

All animal experiments followed the guidelines of the China Animal Authority and the Vision and Ophthalmology Research Society's Statement on the Use of Animals in Ophthalmic and Vision Research. Ethics approval was obtained from Henan Eye Hospital (Permit number: HNEECA-2022-17).

## Author contributions

Haohao Cui: investigation, methodology, and writing – original draft preparation. Bingbing Cui: investigation and methodology. Huiying Chen: investigation and methodology. Xiwen Geng: investigation and methodology. Xingchen Geng: data curation and formal analysis. Zhanrong Li: conceptualization, funding acquisition, project administration, resources, supervision, and validation. Junjie Zhang: validation and methodology. Shaokui Cao: validation and methodology. Jingguo Li: conceptualization, funding acquisition, investigation, methodology, project administration, resources, supervision, validation, and writing – review and editing.

## Conflicts of interest

The authors declare no conflict of interest.

## Acknowledgements

This research was supported by the National Natural Science Foundation of China (52173143), Zhongyuan Thousand Talents Plan Project, and Basic Science Key Project of Henan Eye Institute/Henan Eye Hospital (20JCZD002 and 20JCQN001).

## References

1 Y. Liang, J. He and B. Guo, Functional hydrogels as wound dressing to enhance wound healing, *ACS Nano*, 2021, **15**, 12687–12722.
2 B. Yang, J. Song, Y. Jiang, M. Li, J. Wei, J. Qin, W. Peng, F. L. Lasaosa, Y. He, H. Mao, J. Yang and Z. Gu, Injectable adhesive self-healing multicross-linked double-network hydrogel facilitates full-thickness skin wound healing, *ACS Appl. Mater. Interfaces*, 2020, **12**, 57782–57797.
3 X. Zhao, D. Pei, Y. Yang, K. Xu, J. Yu, Y. Zhang, Q. Zhang, G. He, Y. Zhang, A. Li, Y. Cheng and X. Chen, Green tea derivative driven smart hydrogels with desired functions for chronic diabetic wound treatment, *Adv. Funct. Mater.*, 2021, **31**, 2009442.
4 A. Maleki, J. He, S. Bochani, V. Nosrati, M. A. Shahbazi and B. Guo, Multifunctional photoactive hydrogels for wound healing acceleration, *ACS Nano*, 2021, **15**, 18895–18930.
5 Z. Ming, L. Han, M. Bao, H. Zhu, S. Qiang, S. Xue and W. Liu, Living bacterial hydrogels for accelerated infected wound healing, *Adv. Sci.*, 2021, **8**, 2102545.
6 Z. Ni, H. Yu, L. Wang, X. Liu, D. Shen, X. Chen, J. Liu, N. Wang, Y. Huang and Y. Sheng, Polyphosphazene and non-catechol-based antibacterial injectable hydrogel for adhesion of wet tissues as wound dressing, *Adv. Healthcare Mater.*, 2022, **11**, 2101421.
7 R. Yu, H. Zhang and B. Guo, Conductive biomaterials as bioactive wound dressing for wound healing and skin tissue engineering, *Nano-Micro Lett.*, 2022, **14**, 1.
8 B. Liu, J. Li, Z. Zhang, J. Roland and B. Lee, pH responsive antibacterial hydrogel utilizing catechol-boronate complexation chemistry, *Chem. Eng. J.*, 2022, **441**, 135808.
9 C. Yang, J. Dawulieti, K. Zhang, C. Cheng, Y. Zhao, H. Hu, M. Li, M. Zhang, L. Chen, K. Leong and D. Shao, An injectable antibiotic hydrogel that scavenges proinflammatory factors for the treatment of severe abdominal trauma, *Adv. Funct. Mater.*, 2022, **32**, 2111698.
10 R. Zhang, Y. Tian, L. Pang, T. Xu, B. Yu, H. Cong and Y. Shen, Wound microenvironment-responsive protein hydrogel drug-loaded system with accelerating healing and antibacterial property, *ACS Appl. Mater. Interfaces*, 2022, **14**, 10187–10199.
11 C. L. Dieterich, S. I. Probst, R. Ueoka, I. Sandu, D. Schafle, M. Dal Molin, H. A. Minas, R. Costa, A. Oxenius, P. Sander and J. Piel, Aquimarins, peptide antibiotics with amino-modified c-termini from a sponge-derived Aquimarina sp. Bacterium, *Angew. Chem., Int. Ed.*, 2022, **61**, e202115802.
12 L. Li, B. Koirala, Y. Hernandez, L. W. MacIntyre, M. A. Ternei, R. Russo and S. F. Brady, Identification of structurally diverse menaquinone-binding antibiotics with *in vivo* activity against multidrug-resistant pathogens, *Nat. Microbiol.*, 2022, **7**, 120–131.
13 T. M. Privalsky, A. M. Soohoo, J. Wang, C. T. Walsh, G. D. Wright, E. M. Gordon, N. S. Gray and C. Khosla, Prospects for antibacterial discovery and development, *J. Am. Chem. Soc.*, 2021, **143**, 21127–21142.
14 Y. Yu, J. Li, Y. Zhang, Z. Ma, H. Sun, X. Wei, Y. Bai, Z. Wu and X. Zhang, A bioinspired hierarchical nanoplatform targeting and responding to intracellular pathogens to eradicate parasitic infections, *Biomaterials*, 2022, **280**, 121309.
15 Y. Wang, Y. Yang, Y. Shi, H. Song and C. Yu, Antibiotic-free antibacterial strategies enabled by nanomaterials: progress and perspectives, *Adv. Mater.*, 2019, **32**, 1904106.
16 V. Morya, S. Walia, B. B. Mandal, C. Ghoroi and D. Bhatia, Functional DNA based hydrogels: Development, properties and biological applications, *ACS Biomater. Sci. Eng.*, 2020, **6**, 6021–6035.

17 L. Su, Y. Feng, K. Wei, X. Xu, R. Liu and G. Chen, Carbohydrate-based macromolecular biomaterials, *Chem. Rev.*, 2021, **121**, 10950–11029.
18 J. Yan, Y. Wang, X. Li, D. Guo, Z. Zhou, G. Bai, J. Li, N. Huang, J. Diao, Y. Li, W. He, W. Liu and K. Tao, A bionic nano-band-aid constructed by the three-stage self-assembly of peptides for rapid liver hemostasis, *Nano Lett.*, 2021, **21**, 7166–7174.
19 Y. Jiang, J. Wang, H. Zhang, G. Chen and Y. Zhao, Bio-inspired natural platelet hydrogels for wound healing, *Sci. Bull.*, 2022, **67**, 1776–1784.
20 Y. S. Zhang and A. Khademhosseini, Advances in engineering hydrogels, *Science*, 2017, **356**, eaaf3627.
21 Z. Zhao, Z. Wang, G. Li, Z. Cai, J. Wu, L. Wang, L. Deng, M. Cai and W. Cui, Injectable microfluidic hydrogel microspheres for cell and drug delivery, *Adv. Funct. Mater.*, 2021, **31**, 2103339.
22 L. Sun, Z. Chen, D. Xu and Y. Zhao, Electroconductive and anisotropic structural color hydrogels for visual heart-on-a-chip construction, *Adv. Sci.*, 2022, **9**, 2105777.
23 Z. Ahmadian, A. Correia, M. Hasany, P. Figueiredo, F. Dobakhti, M. R. Eskandari, S. H. Hosseini, R. Abiri, S. Khorshid, J. Hirvonen, H. A. Santos and M. A. Shahbazi, A hydrogen-bonded extracellular matrix-mimicking bactericidal hydrogel with radical scavenging and hemostatic function for pH-responsive wound healing acceleration, *Adv. Healthcare Mater.*, 2021, **10**, 2001122.
24 Z. Qiao, X. Lv, S. He, S. Bai, X. Liu, L. Hou, J. He, D. Tong, R. Ruan, J. Zhang, J. Ding and H. Yang, A mussel-inspired supramolecular hydrogel with robust tissue anchor for rapid hemostasis of arterial and visceral bleedings, *Bioact. Mater.*, 2021, **6**, 2829–2840.
25 Y. Shen, G. Xu, H. Huang, K. Wang, H. Wang, M. Lang, H. Gao and S. Zhao, Sequential release of small extracellular vesicles from bilayered thiolated alginate/polyethylene glycol diacrylate hydrogels for scarless wound healing, *ACS Nano*, 2021, **15**, 6352–6368.
26 X. Zhang, D. Yao, W. Zhao, R. Zhang, B. Yu, G. Ma, Y. Li, D. Hao and F. Xu, Engineering platelet-rich plasma based dual-network hydrogel as a bioactive wound dressing with potential clinical translational value, *Adv. Funct. Mater.*, 2021, **31**, 2009258.
27 L. Zhou, C. Dai, L. Fan, Y. Jiang, C. Liu, Z. Zhou, P. Guan, Y. Tian, J. Xing, X. Li, Y. Luo, P. Yu, C. Ning and G. Tan, Injectable self-healing natural biopolymer-based hydrogel adhesive with thermoresponsive reversible adhesion for minimally invasive surgery, *Adv. Funct. Mater.*, 2021, **31**, 2007457.
28 X. He, L. Dai, L. Ye, X. Sun, O. Enoch, R. Hu, X. Zan, F. Lin and J. Shen, A vehicle-free antimicrobial polymer hybrid gold nanoparticle as synergistically therapeutic platforms for staphylococcus aureus infected wound healing, *Adv. Sci.*, 2022, **9**, 2105223.
29 X. Qi, Y. Huang, S. You, Y. Xiang, E. Cai, R. Mao, W. Pan, X. Tong, W. Dong, F. Ye and J. Shen, Engineering robust Ag-decorated polydopamine nano-photothermal platforms to combat bacterial infection and prompt wound healing, *Adv. Sci.*, 2022, **9**, 2106015.
30 X. He, J. Hou, X. Sun, P. Jangili, J. An, Y. Qian, J. M. Kim and J. Shen, NIR-II photo-amplified sonodynamic therapy using sodium molybdenum bronze nanoplatform against subcutaneous staphylococcus aureus infection, *Adv. Funct. Mater.*, 2022, **32**, 2203964.
31 F. Hu, B. Song, X. Wang, S. Bao, S. Shang, S. Lv, B. Fan, R. Zhang and J. Li, Green rapid synthesis of $Cu_2O$/Ag heterojunctions exerting synergistic, *Chin. Chem. Lett.*, 2022, **33**, 308–313.
32 X. Li, X. Zhao, D. Chu, X. Zhu, B. Xue, H. Chen, Z. Zhou and J. Li, Silver nanoparticle-decorated 2D Co-TCPP MOF nanosheets for synergistic photodynamic and silver ion antibacterial, *Surf. Interfaces*, 2022, **33**, 102247.
33 X. Zhao, X. He, A. Hou, C. Cheng, X. Wang, Y. Yue, Z. Wu, H. Wu, B. Liu, H. Li, J. Shen, C. Tan, Z. Zhou and L. Ma, Growth of $Cu_2O$ nanoparticles on two-dimensional Zr–ferrocene–metal–organic framework nanosheets for photothermally enhanced chemodynamic antibacterial therapy, *Inorg. Chem.*, 2022, **61**, 9328–9338.
34 S. Wu, Y. Yang, S. Wang, C. Dong, X. Zhang, R. Zhang and L. Yang, Dextran and peptide-based pH-sensitive hydrogel boosts healing process in multidrug-resistant bacteria-infected wounds, *Carbohydr. Polym.*, 2022, **278**, 118994.
35 X. Gao, Z. Xu, G. Liu and J. Wu, Polyphenols as a versatile component in tissue engineering, *Acta Biomater.*, 2021, **119**, 57–74.
36 M. Yin, J. Wu, M. Deng, P. Wang, G. Ji, M. Wang, C. Zhou, N. Blum, W. Zhang, H. Shi, N. Jia, X. Wang and P. Huang, Multifunctional magnesium organic framework-based microneedle patch for accelerating diabetic wound healing, *ACS Nano*, 2021, **15**, 17842–17853.
37 F. Wang, M. Liu, C. Liu, Q. Zhao, T. Wang, Z. Wang and X. Du, Light-induced charged slippery surfaces, *Sci. Adv.*, 2022, **8**, eabp9369.
38 X. He, L. Dai, L. Ye, X. Sun, O. Enoch, R. Hu, X. Zan, F. Lin and J. Shen, A vehicle-free antimicrobial polymer hybrid gold nanoparticle as synergistically therapeutic platforms for *Staphylococcus aureus* infected wound healing, *Adv. Sci.*, 2022, **9**, 2105223.
39 X. Qi, Y. Huang, S. You, Y. Xiang, E. Cai, R. Mao, W. Pan, X. Tong, W. Dong, F. Ye and J. Shen, Engineering robust Ag-decorated polydopamine nano-photothermal platforms to combat bacterial infection and prompt wound healing, *Adv. Sci.*, 2022, **9**, 2106015.
40 X. He, J. Hou, X. Sun, P. Jangili, J. An, Y. Qian, J. S. Kim and J. Shen, NIR-II Photo-Amplified Sonodynamic Therapy using sodium molybdenum bronze nanoplatform against subcutaneous *Staphylococcus aureus* infection, *Adv. Funct. Mater.*, 2022, **32**, 2203964.
41 S. Lv, B. song, F. Han, Z. Li, B. Fan, R. Zhang, J. Zhang and J. Li, MXene-based hybrid system exhibits excellent synergistic antibiosis, *Nanotechnology*, 2022, **33**, 085101.
42 Y. Qian, Y. Zheng, J. Jin, X. Wu, K. Xu, M. Dai, Q. Niu, H. Zheng, X. He and J. Shen, Immunoregulation in diabetic

 

wound repair with a photoenhanced glycyrrhizic acid hydrogel scaffold, *Adv. Mater.*, 2022, **34**, 2200521.
43 Y. Qian, Y. Zheng, J. Jin, X. Wu, K. Xu, M. Dai, Q. Niu, H. Zheng, X. He and J. Shen, Immunoregulation in diabetic wound repair with a photoenhanced glycyrrhizic acid hydrogel scaffold, *Adv. Mater.*, 2022, **34**, 2200521.
44 L. Shi, Z. Li, Z. Liang, J. Zhang, R. Liu, D. Chu, L. Han, L. Zhu, J. Shen and J. Li, A dual-functional chitosan derivative platform for fungal keratitis, *Carbohydr. Polym.*, 2022, **275**, 118762.
45 Y. Yang, Y. Liang, J. Chen, X. Duan and B. Guo, Mussel-inspired adhesive antioxidant antibacterial hemostatic composite hydrogel wound dressing via photo-polymerization for infected skin wound healing, *Bioact. Mater.*, 2022, **8**, 341–354.
46 B. Li, L. Shi, R. Liu, Z. Li, S. Cao and J. Li, A lingering mouthwash with sustained antibiotic release and biofilm eradication for periodontitis, *J. Mater. Chem. B*, 2021, **9**, 8694–8707.
47 Y. Liang, Z. Li, Y. Huang, R. Yu and B. Guo, Dual-dynamic-bond cross-linked antibacterial adhesive hydrogel sealants with on-demand removability for post-wound-closure and infected wound healing, *ACS Nano*, 2021, **15**, 7078–7093.
48 H. Tan, Z. Peng, Q. Li, X. Xu, S. Guo and T. Tang, The use of quaternised chitosan-loaded PMMA to inhibit biofilm formation and downregulate the virulence-associated gene expression of antibiotic-resistant staphylococcus, *Biomaterials*, 2012, **33**, 365–377.
49 S. M. Kinney, K. Ortaleza, A. E. Vlahos and M. V. Sefton, Degradable methacrylic acid-based synthetic hydrogel for subcutaneous islet transplantation, *Biomaterials*, 2022, **281**, 121342.
50 Y. Hao, C. Yuan, J. Deng, W. Zheng, Y. Ji and Q. Zhou, Injectable self-healing first-aid tissue adhesives with outstanding hemostatic and antibacterial performances for trauma emergency care, *ACS Appl. Mater. Interfaces*, 2022, **14**, 16006–16017.
51 G. Li, C. Li, G. Li, D. Yu, Z. Song, H. Wang, X. Liu, H. Liu and W. Liu, Development of conductive hydrogels for fabricating flexible strain sensors, *Small*, 2021, **18**, 2101518.
52 P. Bertsch, M. Diba, D. J. Mooney and S. C. G. Leeuwenburgh, Self-healing injectable hydrogels for tissue regeneration, *Chem. Rev.*, 2022, **123**, 834–873.
53 X. Zhao, X. Chen, H. Yuk, S. Lin and G. Parada, Soft materials by design: unconventional polymer networks give extreme properties, *Chem. Rev.*, 2021, **121**, 4309–4372.
54 K. Zhang, Q. Feng, Z. Fang, L. Gu and L. Bian, Structurally Dynamic hydrogels for biomedical applications: Pursuing a fine balance between macroscopic stability and microscopic dynamics, *Chem. Rev.*, 2021, **121**, 11149–11193.
55 L. Su, Y. Feng, K. Wei, X. Xu, R. Liu and G. Chen, Carbohydrate-based macromolecular biomaterials, *Chem. Rev.*, 2021, **121**, 10950–11029.
56 J. Li, L. Zhang, Y. Lin, H. Xiao, M. Zuo, D. Cheng and X. Shuai, A pH-sensitive prodrug micelle self-assembled from multi-doxorubicin-tailed polyethylene glycol for cancer therapy, *RSC Adv.*, 2016, **6**, 9160.
57 J. Sun, M. Li, B. Zhang and X. Chen, High antibacterial activity and selectivity of the versatile polysulfoniums that combat drug resistance, *Adv. Mater.*, 2021, **33**, 2104402.
58 F. Han, L. Shi, Z. Li, L. Jin, B. Fan, J. Zhang, R. Zhang, X. Zhang, L. Han and J. Li, Triple-synergistic 2D material-based dual-delivery antibiotic platform, *NPG Asia Mater.*, 2020, **12**, 15.
59 D. Chen, Q. Tang, J. Zou, X. Yang, W. Huang, Q. Zhang, J. Shao and X. Dong, pH-Responsive PEG-doxorubicin-encapsulated Aza-bodipy nanotheranostic agent for imaging-guided synergistic cancer therapy, *Adv. Healthcare Mater.*, 2018, **7**, 1701272.
60 Z. Guo, L. Shi, H. Feng, F. Yang, Z. Li, J. Zhang, L. Jin and J. Li, Reduction-sensitive nanomicelles: Delivery celastrol for retinoblastoma cells effective apoptosis, *Chin. Chem. Lett.*, 2021, **32**, 1046–1050.
61 Z. Li, R. Liu, Z. Guo, D. Chu, L. Zhu, J. Zhang, X. Shuai and J. Li, Celastrol-based nanomedicine promotes corneal allograft survival, *J. Nanobiotechnol.*, 2021, **19**, 341.
62 L. An, Z. Li, L. Shi, L. Wang, Y. Wang, L. Jin, X. Shuai and J. Li, Inflammation-targeted celastrol nanodrug attenuates collagen induced arthritis through NF-κB and Notch1 pathways, *Nano Lett.*, 2020, **20**, 7728–7736.
63 Y. Zhang, R. Liu, C. Li, L. Shi, Z. Guo, L. Zhu, W. Li, J. Li and Z. Li, Celastrol-based nanomedicine hydrogels eliminate posterior capsule opacification, *Nanomedicine*, 2022, **17**, 1449–1461.
64 B. Cheng, H. Cui, N. Zhang, H. Feng, D. Chu, B. Cui, Z. Li, J. Zhang, S. Cao and J. Li, Antibiotic-free self-assembled polypeptide nanomicelles for bacterial keratitis, *ACS Appl. Polym. Mater.*, 2022, **4**, 7250–7257.
65 Y. Huang, L. Mu, X. Zhao, Y. Han and B. Guo, Bacterial growth-induced Tobramycin smart release self-healing hydrogel for Pseudomonas Aeruginosa-infected burn wound healing, *ACS Nano*, 2022, **16**, 13022–13036.